

In situ-formed cobalt nanoparticles embedded within carbonaceous matrix as highly efficient and selective catalysts for the hydrogenation of nitroarenes

Xiuzheng Zhuang^{1, 2#}, Jianguo Liu^{1, 3*#}, Shurong Zhong¹, Longlong Ma^{1*}

1 CAS Key Laboratory of Renewable Energy, Guangdong Provincial Key Laboratory of New and Renewable Energy Research and Development, Guangzhou Institute of Energy Conversion, Chinese Academy of Sciences, Guangzhou 510640, P. R. China.

2 University of Chinese Academy of Sciences, Beijing 100049, P. R. China.

3 Dalian National Laboratory for Clean Energy, Dalian 116023, P. R. China.

* Corresponding authors e-mail: liujg@ms.giec.ac.cn; mall@ms.giec.ac.cn

These authors contributed equally to this work.

Abstract: Inhibiting the side reactions (such as dehalogenation) while promoting both/transfer hydrogenation are the main target for the production of functional anilines from nitroarenes; consequently, the preparation of an ideal catalyst to improve reaction selectivity stays as the fundamental direction for this field. In this work, we provided an easy-to-prepared heterogeneous catalyst with multilayered graphene shells where cobalt nanoparticles were encapsulated inside and distributed uniformly. This as-prepared catalysts were fabricated via one-pot pyrolysis by using mixture of citrate acid and cobalt acetate as C source and Co source, respectively. First of all, structural features of catalyst were characterized by a series of analytic techniques involving XPS, SEM/EDS, TEM as well as elemental mapping, to reveal its unique properties in relation to the catalytic mechanisms; in simple terms, the outer graphitic shell could be activated by the electronic interaction between the inner metallic nanoparticles and the outer graphene layer. Subsequently, the catalytic performance was tested in hydrogenation of nitrobenzene by using H₂ as hydrogen source, so as to optimize the preparation process as well as the reaction conditions. Other nitro aromatics with functional groups such as halogen atoms, methyl or hydroxyl were also tolerated under very mild industrially viable and scalable conditions (60 °C, 2 h, and 2 MPa H₂). More surprisingly, this catalyst could still exhibit excellent yields over 96 % in gram-scale test for the selected substrates, and could also be easily separated from the aqueous system due to its magnetic properties. The determined yields of target products were not decreased even after eight cycles, suggesting a potential for future industrial application in the selective hydrogenation of nitroarenes to the corresponding amines.

Key words: Cobalt nanoparticle; Graphene-co-shelled structures; Catalytic hydrogenation

1. Introduction

Aromatic amines, as the basic structural blocks of organic compounds, are widely used as precursor in the manufactural industry involving pharmaceuticals, dyestuffs, explosives and agricultural chemicals¹. Among the varied derivatives having aromatic core, aniline is one of the key platform molecule used in different areas, especially for the industrial production of rigid polyurethane foams², whose demands are increasing growth in the recent years. The conventional synthesis of aniline includes an iron powder reduction method and another sulfur reduction method¹⁻³; the former will produce a large amount of iron waste and wastewater while the latter causes serious pollution due to the sulfur itself. As a result, these two methods are being phased out by the industry since more concerns about environmental issues are focused on the chemical industry process. In comparison, catalytic hydrogenation of nitrobenzene using H₂ as the reducing agent to produce aniline is a promising route because of its advantages in terms of efficiency, safe and environmental protection, which usually depends on the metal-based heterogeneous catalysts^{3, 4}. However, most of organic compounds still contain unsaturated functional groups, such as C=C, C=O, and C-Cl (or C-Br, C-I, and C-F, etc.), apart from the nitro groups. These functional groups are easily hydrogenated towards the saturated functional groups or dehalogenated together with the hydrogenation of nitro groups, producing the target products as well as the undesired by-products at the same time, particularly when noble metal catalysts (i.e., Pd, Au, and Pt) with high hydrogenation catalytic activity are used^{5, 6}. In fact, the undesired dehalogenation reaction may become more prominent from C-Cl to C-I bond because of the following reasons^{5, 7, 8}. First of all, the amino groups in the halogenated anilines can function as an electro-donating groups, which promotes the hydrolysis of the C-Cl bond in chloroanilines, making the undesired dehalogenation reaction occur⁸. Additionally, the much weaker C-I bond relative to the C-Cl bond results in the reaction of hydrolysis becoming much easier because of the large atomic diameter as well as low electronegativity of iodine⁷. Thus, selectively reducing the nitro groups on nitroarenes containing other unsaturated or halogenated functional groups to amino groups remains as an important challenge, and then developing an efficient heterogeneous catalyst for the selective hydrogenation of nitroarenes with a wide substrate scope is not only desirable but also highly urgent.

So far, the most frequently used catalysts are scarce noble metals and alloys which inevitably impedes the large-scale application as their cost, and the substitution of such costly precious-metal catalysts with earth-abundant available transition-metal catalysts holds enormous promise for the conversion of nitroarenes into the corresponding anilines. Additionally, the features of easy separation and recycling of catalysts are also critical for the practical applications since the synthesis process takes place mainly in the aqueous system. For this reason, lots of efforts have been turned into transition metals, such as cobalt (Co) and Co-based materials, because they possess many superior properties such as environmental friendliness, good performance, and

ferromagnetic properties at room temperature, which are actively pursued in the preparation of heterogeneous catalysis^{5, 6, 8-10}. Unfortunately, Co-based nanoparticles or its metallic oxides are susceptible to agglomerate during usage owing to their high surface energy and high reactivity⁹, and the leaching of metallic atoms in aqueous systems after reaction are another challenge for industrial application^{5, 10}. Both of these drawbacks deteriorate its catalytic activity and selectivity during the process of hydrogenation. To overcome the above limitations, increasing researchers have turned their attentions to the porous supports with higher surface area as it contributes to disperse the active metals and stabilize the metallic nanoparticles, such as SiO₂^{1, 11}, MOF³, and carbonaceous matrix like C₆₀ or graphene¹². For instance, Beller et al.^{13, 14} demonstrated that the halogenated nitrobenzenes could be completely transformed into the corresponding anilines over cobalt-phenanthroline complexes derived Co oxide-N/C catalyst under 5 MPa H₂ at 110 °C. Similarly, Wang et al.¹⁵ illustrated that the Co/Co₃O₄@NCNTs catalyst exhibited good to excellent catalytic performance for the hydrogenation of substituted nitrobenzenes with a wide scope under 3 MPa H₂ at 110 °C. Alex et al.¹⁶ also encapsulated Co in polymer EnCatTM, and employed it in the selective hydrogenation of iodine-containing aromatics under high temperature and H₂ pressure. All of them confirm that the small sized and uniformly distributed metal active centers could be reached in their experiments, which might greatly increase the catalytic activity for nitrobenzene hydrogenation; however, several defects still exist in most of the synthesis procedures, such as the complicated processes, relatively large catalyst dosage, and harsh reaction conditions. Consequently, an easier system of heterogeneous transition-metal catalyst preparation is necessary for the production of functional anilines, which severs to optimize the actual efficiency in industrial production.

Herein, we explored a simplified method for the preparation of graphene shell encapsulated metallic nanoparticles, in fewer easily practical synthetic steps with low energy consumption¹⁷. Importantly, the method was environmental friendly as it employs EtOH in its aqueous system, which makes the presented protocol safer in comparison with the previously reported procedure in which highly dangerous solvent was used. Another advantage from the use of EtOH reflects in the uniformly mixing of cobalt acetate (as cobalt source) and citrate acid (as carbon source) prior to the pyrolysis step, leading to a well-distributed of metallic atoms in carbonaceous matrix. The structural features of catalysts associate with its catalytic activity were characterized by several techniques, and the selected catalysts were next applied to the challenging hydrogenation of nitrobenzene for the synthesis of aniline under varied conditions. Subsequently, with the optimized conditions in hands, we conducted the synthesis of more than 27 samples of nitroarenes for the corresponding anilines with varied functional groups. Last but not least, we have also demonstrated the hydrogenation protocol to gram-scale synthesis as well as lifecycle performance in batch reactor to prove the potential in industrial application, which can provide an available preparation of simple but highly efficient catalysts for the hydrogenation of nitroarenes in near future.

2. Experimental section

2.1 Methods and materials

The chemicals and solvents used in this study were purchased from the certified companies registered in China Academy Science On-line market systems. For instance, 1,3,5-trimethoxybenzene was purchased from Sigma Aldrich Co., Ltd.; $\text{Co}(\text{CH}_3\text{CO}_2)_2 \cdot \text{H}_2\text{O}$ (AR, 98 %), anhydrous citric acid¹⁸, CDCl_3 (99.8 % D, stabilized with Ag) were obtained from Shanghai Macklin Biochemical Co., Ltd.; H_2SO_4 (GR, 98 %) was purchased from Sinopharm Chemical Reagent Co., Ltd.; methanol (AR, 99.7 %) and ethanol (GC, > 99.9 %) were purchased from Aladdin (Shanghai) Chemical Technology Co., Ltd.; Deionized water ($\sigma < 5 \mu\text{S/m}$) was self-made in the laboratory by a water purification machine; the nitro substrates were obtained commercially from various chemicals companies, but all of them were checked for the purity prior to experiments.

2.2 General preparation and analysis of catalysts

Briefly, cobalt acetate ($\text{Co}(\text{CH}_3\text{CO}_2)_2 \cdot \text{H}_2\text{O}$, 0.03 mol) and citric acid ($\text{C}_6\text{H}_8\text{O}_7$, 0.03 mol) were dissolved in anhydrous ethanol (5 ml). The mixture was then aged at 70 °C for about 6 h under constant stirring (300 rpm) to obtain a bubble-shaped pinkish gel, followed by drying at 100 °C for 24 h in an electric oven to remove the excess solvent. Subsequently, this pinkish solid was then pyrolyzed at 600 °C for 3 h under a high-purity N_2 (99.999 %) flow of 40 mL/min, whose heating rate was controlled at 5 °C/min. The obtained solid was identified as Co-based catalyst, which was further rinsed with the 1 M H_2SO_4 and H_2O to remove the unloaded metals and readjust the pH of catalyst back to 7, respectively. Finally, a cobalt nanoparticles encapsulated in graphene layer ($\text{Co}@C$) catalyst could be obtained after vacuum freeze-drying at -41 °C overnight. Some of $\text{Co}@C$ catalysts were further oxidized under O_2/Ar (5% O_2 in Ar, 99.999% purity) atmosphere at 200 °C for 2 h to provide the $\text{Co}/\text{CoO}@C$ catalyst, which is helpful to distinguish the catalytic properties between metallic atoms and oxides. All of these materials were labeled as $\text{Co}@C$ - x - y or $\text{Co}/\text{CoO}@C$ - x - y , where x suggests the pyrolysis temperature, and y denotes the solvent.

The obtained catalysts were characterized by its structural features in relation to carbonaceous matrix and catalytic properties. The TEM measurements were conducted on a JEM-2100F microscope (JEOL, Japan) operated at 200 kV to observe the distribution of metallic atoms, The SEM images were obtained on an analytical SEM SU-70 (Hitachi, Japan) microscope operated at 10 kV, which was coupled with an energy dispersive X-ray spectrometry (EDS; Thermo Scientific, Waltham, MA) to measure the relative content of metallic atoms. In addition, XPS analysis was performed on an Escalab250 Xi photoelectron spectrometer (Thermo Fisher Scientific, America) under $\text{Al K}\alpha$ X-ray radiation with a scan number of 25, which could help to identify the surface functionalities of catalysts and its variation under different processing conditions. For the cobalt functionalities^{9, 19, 20}, characteristic peaks were located in the range of 778-783 eV ($\text{Co } 2p_{3/2}$) and

793-798 eV (Co 2p_{1/2}) with specific forms of Co⁰ and Co²⁺ (i.e., CoO, Co(OH)₂). For the carbon functionalities^{21, 22}, characteristic peaks could be identified corresponding to: 1) -C-H (283.5 ± 0.3 eV); 2) -C-(C, H)/C=C (284–285 eV); 3) -C-(O, N) (286.1 ± 0.2 eV); 4) -C=O (287.6 ± 0.3 eV), and 5) -O=C-O (289.1 ± 0.4 eV). For the oxygen functionalities, characteristic peaks could also be found at around: 1) inorganic oxygen (530.0 ± 0.3 eV); 2) -C-O (531.4 ± 0.3 eV); 3) -C=O (532.8 ± 0.3 eV), and -COOH (533.2 ± 0.3 eV).

2.3 Procedure for the hydrogenation of nitroarenes

The hydrogenation of nitroarenes was carried out in a stainless-steel autoclave (Anhui Kemi Machinery Technology Co., Ltd, China) coupled with several holes, a thermocouple, and a system of recirculating cooling water. Each hold can contain a glass lining with volume of around 10 ml, in which a mixture of 0.5 mmol substrates, 0.05 mmol 1,3,5-trimethoxybenzene, 10 mg catalyst, and 5 ml MeOH were loaded together for the hydrogenation reaction. Afterwards, the autoclave was sealed and purged with 2 MPa H₂ for at least three time to remove the residual air inside, and the magnetic rotor was set at 300 rpm throughout the whole reaction period to ensure the homogeneous heating. The autoclave was preheated from room temperature to target temperature at a constant rate of 2 °C/min, and hold for a certain time for the complete hydrogenation of reactants. Once the reaction was finished, the autoclave was cooled down to ambient temperature, and the target products in aqueous mixture was filtered and primarily identified by GC-MS (Thermo Fisher Scientific, America) with a TG-5MS column (30 m × 250 mm × 0.25 μm). The yields of the target products were further determined by ¹H NMR on a Bruker Avance III spectrometer (Bruker BioSpin, Germany) using 1,3,5-trimethoxybenzene as internal standard; during the analysis of ¹H NMR, about 2 mL filtrate were concentrated by rotary evaporation systems, which was further dissolved in 6 mL CDCl₃ (pre-neutralized with basic Al₂O₃) prior to analyze.

3. Result and discussion

3.1 Catalysts properties

Initially, the morphological structures of catalysts were investigated by means of SEM, TEM, and EDS techniques, whose results were depicted in Fig.1. According to the SEM images, the prepared catalysts had a sponge-like structure and was strongly affected by the pyrolysis temperature. Clearly, higher temperature accelerated the release of organic matter in forms of gaseous mixtures (i.e., CO₂, H₂O, CH₄, and C₂-C₄), which led to the relatively smooth surface on Co@C-500-EtOH becoming rather rough and fragile on that of Co@C-700-EtOH²³. In the meanwhile, direct pyrolysis in an inert gas atmosphere would also transferred the Co²⁺ species into metallic cobalt. Pei et al.²⁰ suggested that these porous surface of the carbonaceous matrix was beneficial for the intimate and dense crosslinking of metallic atoms, but interestingly the cobalt content was slightly reduced from 11.8 % at Co@C-600-EtOH to 9.7 % at Co@C-700-EtOH based on the EDS results.

This trend might be attributed to fact that much more metallic atoms were exposed on the surface of carbonaceous matrix caused by the excess devolatilization at higher pyrolysis temperature, which were easily washed off by acid in the post-treatment²⁴. On the other hand, the magnified TEM analysis of prepared catalysts in Fig.1 (d)-(f) revealed the formation of cobalt nanoparticles, whose average sizes were slightly shifted from 7.1 nm at Co@C-500-EtOH to 9.4 nm at Co@C-700-EtOH, indicating that the increase of pyrolysis temperature induced aggregation of cobalt to larger nanoparticles. In addition, most of them were surrounded by a combination of some graphitic layers and short-range ordered graphitic shells, as the cobalt nanoparticles that loosely bonded on the surface of carbonaceous matrix were washed off with acid²⁵. In the Co@C-500-EtOH, amount of metallic atoms was present in the core-shell structures, and no obvious formation of graphitic shells was observed. By increasing pyrolysis temperature, Co@C-600-EtOH and Co@C-700-EtOH contained more metallic atoms, and incipient formation of graphitic shells enveloping the metallic atoms was evident, as shown in Fig. S1. Apparently, this structural variation is crucial for high activity and stability of catalysts as the metallic atoms should be accessible to reactants and performed as active center for catalytic reaction²⁶. The porous structure of catalysts could be clearly seen in the magnified region of TEM in Fig. S1 as well. Several nano-scale pores were distributed homogeneously through the whole graphene shells, allowing the efficient diffusion, transportation and transfer of reactants to the catalytic active sites. In the Co@C-600-EtOH, cloudy regions of carbon, oxygen, and cobalt species in the 1- to 2-nm range were also detected via the corresponding elemental mapping images (as shown in Fig.1(g)-(j)), which is in good agreement with the TEM results. The coexistence of carbon and cobalt illustrated the complete encapsulation of metallic atoms by graphene shells, while the presence of oxygen species could be caused by the superficial oxidation of cobalt in air, consistent with the observations on Co-based catalysts previously reported^{9, 26}. The uniform distribution of these elements through the whole carbonaceous matrix was also observed, indicating the suitable procedure during the preparation processes.

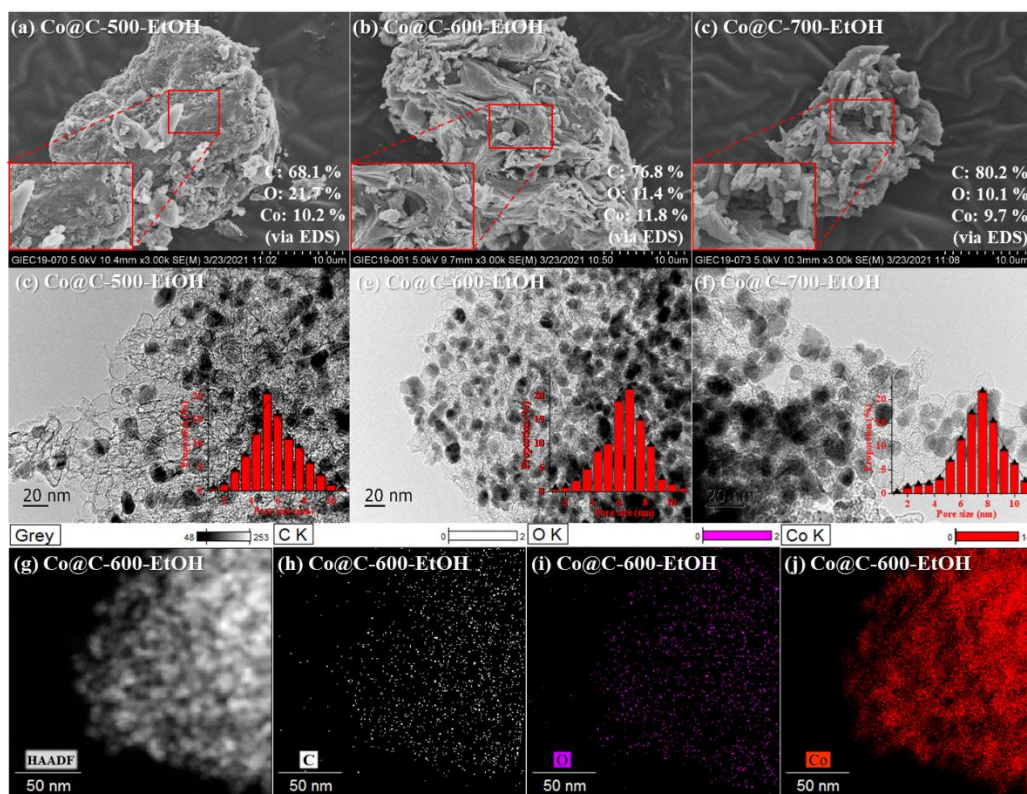


Fig.1 SEM (a, b, and c) and TEM (d, e, and f) images of the prepared catalysts under different pyrolysis temperatures, and the corresponding elemental mapping (g, h, i and j) image of Co@C-600-EtOH.

In attempt to obtain insights into the chemical states of surface elements involving carbon, oxygen and cobalt functionalities, the relevant spectra together with its variation under different conditions had been explored by XPS technique. The high resolution spectrum of C 1s was shown in Fig.2 (a), where five signals at 283.6 eV, 284.8 eV, 286.1 eV, 287.5 eV and 289.5 eV were respectively identified as -C-H (i.e. C bound to H), -C-(C, H)/C=C (i.e. C doubly bound to C or singly bound to C or H), -C-(O, N) (i.e. C bound to C or N), -C=O (i.e. C doubly bond to O) and O-C=O (i.e. C singly and doubly bound to O) for all the prepared catalysts^{21, 22}. Among them, -C-(C, H)/C=C was the predominant carbon functionalities since its highly graphitic structures after pyrolysis, which would further be improved from 48.3 % to 64.7 % with the increase of temperature. At the same time, other carbon functionalities connected with oxygen, such as -C-O, -C=O and O-C=O, suffered from slightly decrease due to the devolatilization process. This phenomenon was also in accord with the O 1s spectra as shown in Fig.2 (b), where the first peak at 530.2 eV was representative of a cobalt oxide network while the following peaks at 531.6 eV (i.e., -C-O), 532.5 eV (i.e., -C=O) and 533.6 eV (i.e., -COOH) could be related to the presence of hydroxyl and carboxyl groups in the inner surface. Further, although the cobalt content determined by EDS provide a comparable result with that of oxygen, the XPS peak intensity of metallic nanoparticles was relatively weak for the prepared catalysts. The reason should be that metallic nanoparticles were embedded in the graphene shells, which was difficult to be detected by XPS since it can only measure the valence state of the surface sites^{8, 24}. However, the characteristic peaks within

the range of Co 2p spectra could still be deconvoluted in Fig.2 (c), where the Co 2p_{3/2} peaks centered at 778.8 eV, 780.9 eV, and 783.1 eV corresponded to the Co⁰, Co²⁺, and Co(OH)₂ species, respectively²⁰. Similarly, the peaks with the binding energies of 793.9 eV, 795.9 eV, and 798.2 eV in Co 2p_{1/2} region were also ascribed to the Co⁰, Co²⁺, and Co(OH)₂ species, respectively. The percentage of Co⁰ increased from 23.8 % to 36.6 % with an increase of pyrolysis temperature of 500-600 °C, but decreased to 28.2 % when the temperature was further up to 700 °C. Obvious positive shift of Co 2p binding energy was also observed at higher pyrolysis temperature, and weaker peak belonging to Co⁰ could be detected. In addition, two peaks were assigned to the “shake-up” corresponding to the excitation of multielectron⁹. With a small amount of Co(OH)₂ on the surface of the catalysts, the cobalt species were mainly in the form of metallic cobalt and cobalt oxide, and the content of metallic cobalt is slightly higher than that of cobalt oxide^{19, 25}. Furthermore, the ration of CoO/Co⁰ on the surface of Co@C-500-EtOH was higher than that on the surface of Co@C-600-EtOH and Co@C-700-EtOH. This was because Co@C-500-EtOH was with small size, and the proportion of unsaturated cobalt in Co@C-500-EtOH was also larger; as a result, cobalt on the surface of the Co@C-500-EtOH get easily oxidized in air.

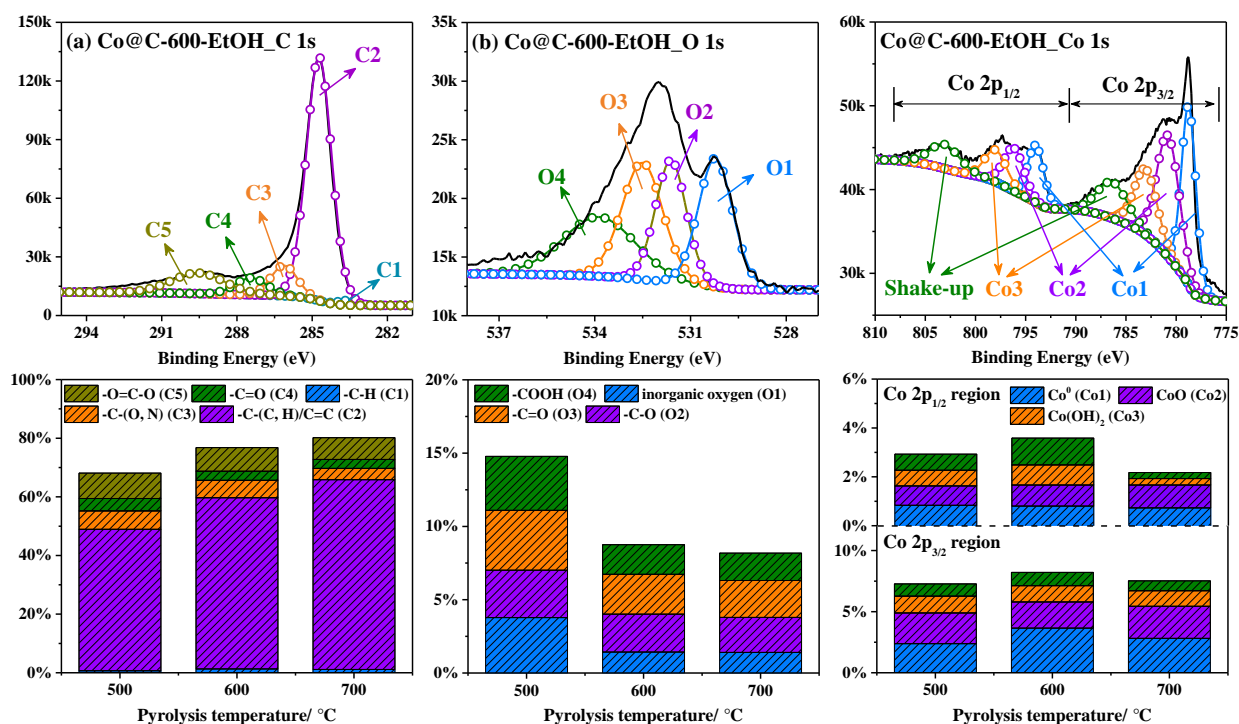


Fig.2 The XPS spectra associated with the C 1s (a), O 1s (b), and Co 2p (c) species of the prepared catalysts, and their variation after different pyrolysis temperatures.

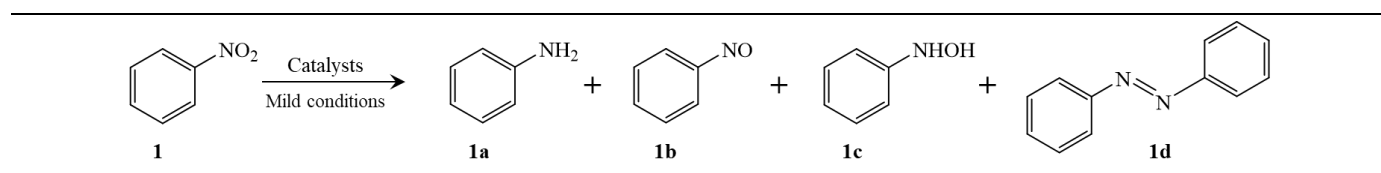
3.2 Catalysts performance

In this section, the hydrogenation of nitrobenzene towards aniline (i.e., **1a**) is one of the most common model reactions^{1, 14}, which is used to gain more information into the relationship between structural features and their catalytic performance. Generally speaking, except for the target product (i.e., **1a**), nitrobenzene presents a complex reaction containing many intermediates or by-products, such as nitrosobenzene (i.e., **1b**), N-phenylhydroxylamine (i.e., **1c**), and azobenzene (i.e., **1d**)¹. So that, the selective hydrogenation of

nitrobenzene over various Co-based catalysts as well as different conditions were performed, whose results were clearly illustrated in Table 1. The entry of 1-3 exhibited the conversion and selectivity of nitrobenzene as a function of pyrolysis temperatures, indicating that all of the prepared catalysts could completely convert nitrobenzene but the selectivity towards aniline was in an order of Co@C-600-EtOH (98.4 %) > Co@C-500-EtOH (93.7 %) > Co@C-700-EtOH (14.4 %). It is also worth noting that according to the TEM results, the catalysts with smaller sizes did perform relatively well, which is agreement with the generally accepted concept that the metallic atoms with high dispersion normally exhibit superior catalytic activity⁸. The use of EtOH could improve the catalytic selectivity for aniline when compared to the catalysts prepared in H₂O (Entry 2, 4); however, the introduction of oxygen atoms during oxidation step significantly decreased the catalytic selectivity for aniline (Entry 5). It can be concluded that the best catalyst according to our experimental procedure is Co@C-600-EtOH, whose catalytic activity and selectivity to yield aniline reach more than 99 % and 98 %, respectively. The hydrogenation activity of Co@C-600-EtOH was comparable to those of Co-based and other catalysts in previous studies^{27, 28}, which could be related to the positive effect of metallic nanoparticles on the carbonaceous matrix as previous studies had proven that the porous nature of carbonaceous matrix was conducive to mass transfer and catalytic activity²⁹. No evident by-products were detected in this catalytic system, suggesting that an adequate ability of catalyst may be involved in the hydrogenation of nitrobenzene to aniline. In comparison to the as-prepared catalysts, use of commercial Raney Co afforded a yield of 99.0 % for aniline while Raney Ni only yield 87.1 %. On the other hand, most of noble-based catalysts exhibited a relatively lower selectivity for nitrobenzene hydrogenation, corresponding to 21.8 %, 94.1 %, 0.0 %, and 80.1 % for 5 % Ru/C, 5 % Pt/C, 5 % Pt/C, and 5 % Pd/C, respectively.

From these results, the selective hydrogenation of nitrobenzene can be successfully done, and the optimization of processing conditions involving reaction temperatures, holding period, H₂ pressure, and the amount of catalyst were simultaneously evaluated based on the Co@C-600-EtOH catalyst. It could be seen that considerable yield of aniline (96.6%, Entry 13) was achieved even at 60 °C without other notable by-products, but further decreasing reaction temperature (Entry 12) or amount of catalyst (Entry 15, 16) obviously led to the reduction of catalytic selectivity. Other factors such as holding period and H₂ pressure reflected similar influences (Entry 17-19). In summary, the selective hydrogenation of nitrobenzene catalyzed by Co@C-600-EtOH can reach its best result under the optimized conditions at 60 °C, 2 h, 10 mg catalysts, and 2 MPa H₂ pressure.

Table 1 Selective hydrogenation of nitrobenzene over different catalysts and conditions



| Entry | Catalysts | Conv. / % | Yield of 1a / % | Entry | Catalyst | Conv. / % | Yield of 1a / % |
|----------|---------------------------|--------------|---------------------------|-----------|----------|--------------|---------------------------|
| 1 | Co@C-500-EtOH | > 99 | 93.7 | 6 | 5 % Ru/C | > 99 | 21.8 |
| 2 | Co@C-600-EtOH | > 99 | 98.4 | 7 | 5 % Pt/C | > 99 | 94.1 |
| 3 | Co@C-700-EtOH | > 99 | 14.4 | 8 | 5 % Rh/C | > 99 | 0.0 |
| 4 | Co@C-600-H ₂ O | > 99 | 60.0 | 9 | 5 % Pd/C | > 99 | 80.1 |
| 5 | Co/CoO@C-600-EtOH | > 99 | / | 10 | Raney Co | > 99 | 99.0 |
| / | / | / | / | 11 | Raney Ni | > 99 | 87.1 |

| Entry | Catalysts | Reaction conditions | Conv./ % | Yield of 1a / % |
|-----------|---------------|--|----------|------------------------|
| 12 | Co@C-600-EtOH | 50 °C, 2 h, 10 mg catalysts, and 2 MPa H ₂ | > 99 | 46.6 |
| 13 | | 60 °C, 2 h, 10 mg catalysts, and 2 MPa H ₂ | > 99 | 96.6 |
| 14 | | 80 °C, 2 h, 10 mg catalysts, and 2 MPa H ₂ | > 99 | 98.4 |
| 15 | | 60 °C, 2 h, 5 mg catalysts, and 2 MPa H ₂ | > 99 | 48.3 |
| 16 | | 60 °C, 2 h, 7.5 mg catalysts, and 2 MPa H ₂ | > 99 | 70.5 |
| 17 | | 60 °C, 1 h, 10 mg catalysts, and 2 MPa H ₂ | > 99 | 55.7 |
| 18 | | 60 °C, 2 h, 10 mg catalysts, and 1 MPa H ₂ | > 99 | 39.0 |
| 19 | | 60 °C, 1 h, 10 mg catalysts, and 4 MPa H ₂ | > 99 | 53.2 |

Note: Screening of prepared and commercial catalysts are based on the below conditions: 80 °C, 2 h, 10 mg catalyst, 5 ml MeOH, 2 MPa H₂, and 0.5 mmol nitrobenzene; the best catalyst was selected to further optimize the reaction conditions. Yields and conversion were determined by GC-MS and ¹H NMR spectroscopy using 1,3,5-trimethoxybenzenes as an internal standard.

With the optimal reaction conditions in hand, the general scope of the Co@C-600-EtOH catalyst was subsequently investigated for the selective hydrogenation of various nitro-containing compounds. As given in Fig.3, this catalyst could convert most of substituted nitrobenzenes towards the corresponding amines with excellent yields and selectivity, reflecting great potential in the industrial application. When the substituents on the aromatic ring of nitrobenzenes were methyl, ethyl, or ether groups (Entry 20-26), the overall conversion efficiency was slightly better than that of halogenated nitrobenzenes. This phenomenon might be caused by the fact that these groups were electron-donating group, quite favorable for the selective hydrogenation on the benzene ring^{3, 27}. To some extent, halogen-substituted nitrobenzenes can also be reduced to halogenated anilines in good to excellent yields over 92 %, known as an essential agrochemical intermediate with high yield and no dehalogenation (Entry 27-30). All ortho-, meta-, and para-group nitrobenzenes were converted rapidly and completely, revealing that slight steric hindrance to the hydrogenation of the nitro groups could be well tolerated⁴. More importantly, for multi-halogen substituted nitrobenzenes, such as 4-Br-1-F-2-nitrobenzene (Entry 31), 3-Cl-2,4-difluoronitrobenzene (Entry 32), 2-Br-4-fluoronitrobenzene (Entry 33), 2-Cl-4-fluoronitrobenzene (Entry 34), and 5-Cl-2-nitrobenzotrifluoride (Entry 35), the reaction only could yield 83 %, 85 %, 86 %, 82 %, and 90 % of the target products, respectively. Increasing reaction temperatures to 80 °C was helpful to induce the occurrence of hydrogenation for some multi-halogen substituted nitrobenzenes

in excellent yields (Entry 36-40). Other halogenated or methyl substitutes dangled on the heterocycle aromatics (i.e, pyridine, indole) were also tolerated in our experiments (Entry 41-43). In addition, hydroxyls as sensitive functional groups are well preserved in our catalytic systems (Entry 44, 45), among which the nitro groups were successfully converted to the corresponding amino groups with an excellent yield. It was interesting because Song et al.²⁷ reported that the electron-donating effect of hydroxyl groups would lead to the difficult polarization of nitro group. Finally, three substrates were selected for the selective hydrogenation at the gram scale (Entry 27-29), and all of them were similar to those small-scale reactions by exhibiting excellent yields of the corresponding products.

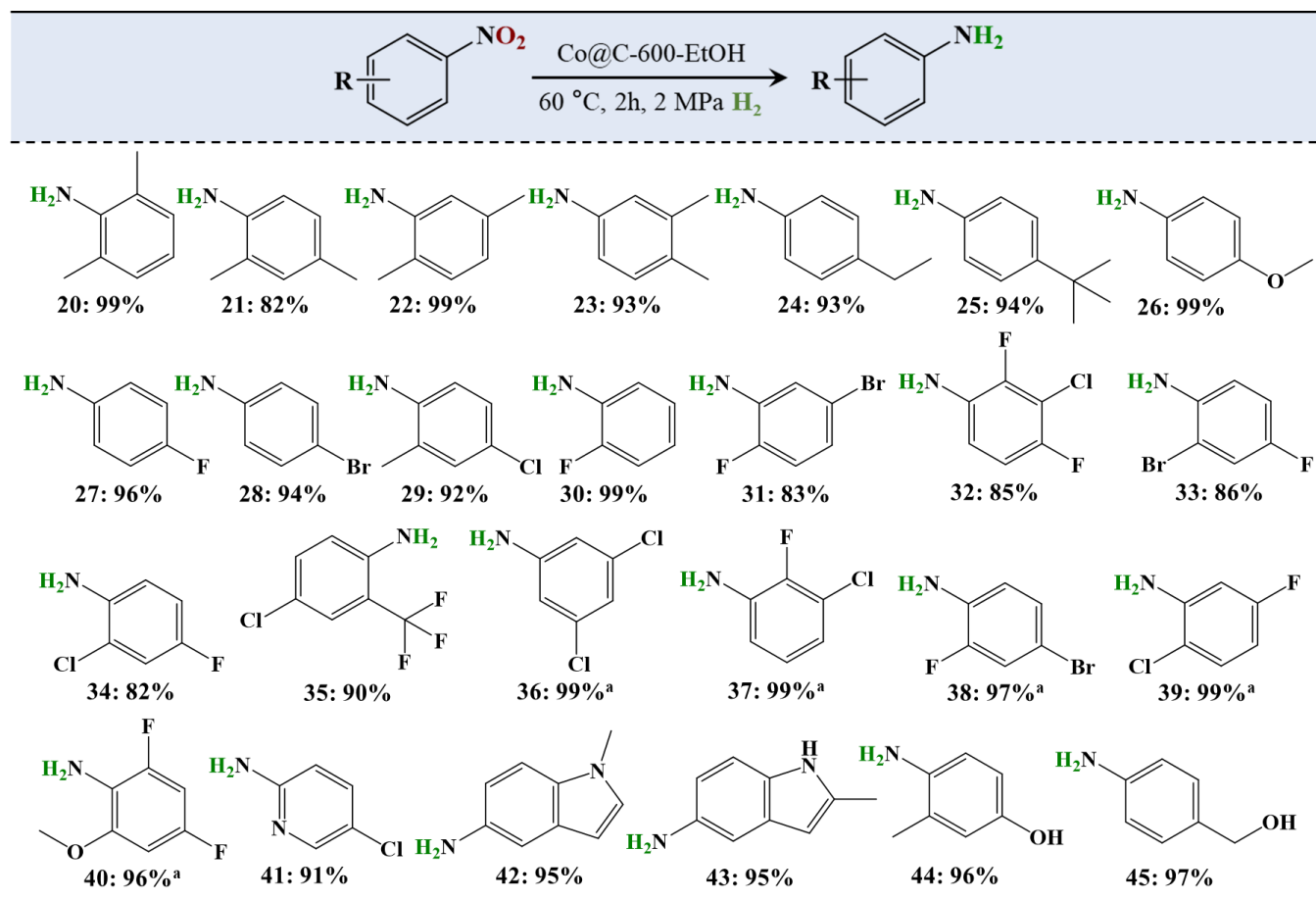
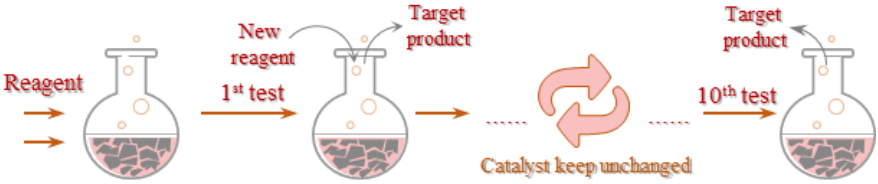


Fig.3 Selective hydrogenation of functional nitroarenes catalyzed by Co@C-600-EtOH. Reaction condition: 60 °C, 2 h, 10 mg catalyst, 5 ml MeOH, 2 MPa H₂, and 0.5 mmol substrates. Yields and conversion were determined by GC-MS and ¹H NMR spectroscopy using 1,3,5-trimethoxybenzenen as an internal standard. ^a Reaction temperature increased to 80 °C.

In terms of the reusability of catalyst, we next performed the selective hydrogenation of nitrobenzene using Co@C-600-EtOH under the identical conditions in successive runs as shown in Table.2, where Raney Co was also adopted as a commercial catalyst for reference. Firstly, due to the magnetic property held by the Co-based catalysts, both of them could be easily separated from the aqueous systems by a magnetic bar, which is considered as an advantage in the industrial application. Secondly, the reusability of our graphene-shelled catalysts was proven to be superior since it showed the excellent catalytic activity and selectivity over 96 %

even after eight cycles; in contrast, the catalytic activity for Raney Co was well maintained, but the catalytic selectivity for target products was significantly reduced from 95.6 % at the first cycle to 42.3 % at the eighth cycle. This might be caused by the graphene shells of Co@C-600-EtOH which fully encapsulate the metallic nanoparticles and thereby physically isolating them from leaching into the aqueous environment.

Table 2 Recycling test of the Co@C-600-EtOH and commercial catalyst.



| Cycle | Catalysts | Conv. / % | Yield of aniline/ % | Cycle | Catalyst | Conv. / % | Yield of aniline/ % |
|-----------------|---------------|-----------|---------------------|-----------------|----------|-----------|---------------------|
| 1 st | Co@C-600-EtOH | > 99 | 96.5 | 1 st | Raney Co | > 99 | 95.8 |
| 2 nd | | > 99 | 96.2 | 2 nd | | > 99 | 95.6 |
| 3 rd | | > 99 | 96.4 | 3 rd | | > 99 | 83.9 |
| 4 th | | > 99 | 95.9 | 4 th | | > 99 | 72.8 |
| 5 th | | > 99 | 96.1 | 5 th | | > 99 | 70.2 |
| 6 th | | > 99 | 96.7 | 6 th | | > 99 | 71.2 |
| 7 th | | > 99 | 96.2 | 7 th | | > 99 | 61.8 |
| 8 th | | > 99 | 97.4 | 8 th | | > 99 | 42.3 |

Reaction condition: 60 °C, 2 h, 10 mg catalyst, 5 ml MeOH, 2 MPa H₂, and 0.5 mmol nitrobenzene. Yields and conversion were determined by GC-MS and ¹H NMR spectroscopy using 1,3,5-trimethoxybenzenen as an internal standard.

Last but not least, we proposed the functional mechanism of Co@C-600-EtOH on catalyzing the selective hydrogenation of nitroarene with H₂ as H source. In this reaction process depicted in Fig.4, the catalytic performance of catalyst was depended on the adsorption behavior of nitroarene on the active sites^{1, 5, 8, 9, 28, 30}. Initially, the electrons of H₂ transferred across the interface of metallic nanoparticles which functioned as an electronic transmission medium, and then the H₂ dissociated to form two adsorbed hydrogens (H·). These adsorbed hydrogens reacted with the adsorbed nitro group to form nitrosoarene, who would further react with the adsorbed hydrogen to produce the hydroxylamine. Afterwards, the transition state of hydroxylamine with adsorbed hydrogens converted to aniline by losing a H₂O molecule, which was desorbed into the aqueous environment. Finally, aniline was also desorbed from the catalyst surface, providing an active site for the next catalytic cycle. The above mention belonged to the direct pathways of nitroarene hydrogenation, and the whole process was completely on the surfaces of metallic nanoparticles wrapped with graphene shells. However, another indirect pathway might also exist on the basis of previous studies^{5, 30}. Two of the intermediates (i.e., nitrosoarene, and hydroxylamine) could undergo condensation reactions to form the azoxyarene intermediates, while the subsequent pathway of the hydrogenation process was followed by the reduction of azoxyarene and azoarene. According to the results reported by Wu et al.⁵ and Han et al.³⁰, the indirect pathway was more

possible for the hydrogenation process catalyzed by Co- or Ni-based catalysts while the other transition metal such as Fe preferred to the direct pathway. Tian et al.²⁸ also provided the DTF results for the selective hydrogenation of nitrobenzene to support the above mechanisms.

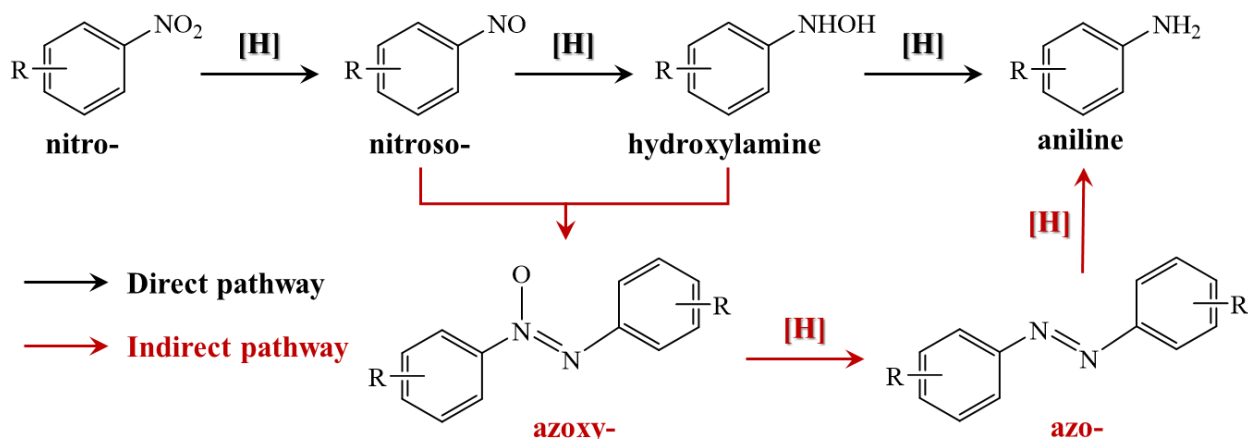


Fig.4 The possible reaction pathways of the selective hydrogenation of nitrobenzene

4. Conclusion

In summary, we have successfully used the prepared catalysts of Co@C-600-EtOH on the selective hydrogenation of nitroarenes, and indicate that a series of functionalized nitroarenes (more than 27 samples) were synthesized in good to excellent yield (80-99 %) under mild industrially viable and scalable condition (i.e., 60 °C, 2 h, and 2 MPa H₂). This protocol could also exhibit a similar reactivity during the gram-scale as well as possess a longer lifecycle without any significant loss of catalytic activity in contrast to the commercial catalysts. According to its structural features, it can be found out that Co²⁺ in the structure of graphene shells is reduced during the pyrolysis process to metallic cobalt, and that the final size of the formed nano-scale particles could be controlled by varying the pyrolysis temperature. At the same time, these nanoparticles facilitate the formation of graphitic layers surrounding the metallic atoms which promoted the free diffusion of reactant towards the catalyst surface and inhibited the aggregation of the metallic nanoparticles. Moreover, the attachment of graphene shell to the nanoparticle surface could calm down the oxidation processes of metallic atoms and improve the stability of catalysts, which was more beneficial for the separation and possibly recycling of the catalyst. The above findings strongly confirm an available and the feasible preparation of simple but highly efficient catalysts towards selective hydrogenation of nitroarenes. By and large, the advantages of this newly developed and simplified method was recommended for the synthesis of functional aniline, as well as the highly efficient and industrial applicable tandem synthesis process.

Acknowledgment This work was supported financially by the National Key R&D Program of China (2018YFB1501500), National Natural Science Foundation of China (51976225), DNL Cooperation Fund, and

Chinese Academy of Sciences (DNL201916).

Author contributions J. G. L. and L. L. M supervised and designed the research. X. Z. Z. performed most of the pre-experiments and data analysis. S. R. Z. performed substrates scope experiments. Z.X.Z. wrote the paper. J.G.L. reviewed and wrote the original manuscript. All authors discussed the results and assisted during manuscript preparation.

Competing interests The authors declare no competing financial interests.

Additional information Correspondence and requests for materials should be addressed to L. L. M or J. G. L.

Reference

1. B. Zhao, Z. Dong, Q. Wang, Y. Xu, N. Zhang, W. Liu, F. Lou and Y. Wang, *Nanomaterials*, 2020, **10**, 883.
2. S. Tadrent, A. Khelfa and C. Len, *Sustainability*, 2020, **12**.
3. H. J. Pan, Y. Y. Peng, X. H. Lu, J. He, L. He, C. L. Wang, F. F. Yue, H. F. Zhang, D. Zhou and Q. H. Xia, *Molecular Catalysis*, 2020, **485**, 9.
4. S. Chen, L. L. Ling, S. F. Jiang and H. Jiang, *Green Chemistry*, 2020, **22**, 5730-5741.
5. W. Wu, W. Zhang, Y. Long, J. H. Qin and J. T. Ma, *Molecular Catalysis*, 2020, **497**, 10.
6. M. Pietrowski, M. Zielinski, E. Alwin, I. Gulaczyk, R. E. Przekop and M. Wojciechowska, *Journal of Catalysis*, 2019, **378**, 298-311.
7. Y. M. A. Yamada, S. M. Sarkar and Y. Uozumi, *J Am Chem Soc*, 2012, **134**, 3190-3198.
8. Y. L. Cao, K. K. Liu, C. Wu, H. P. Zhang and Q. Y. Zhang, *Applied Catalysis a-General*, 2020, **592**, 9.
9. Y. Xu, W. X. Shan, X. Liang, X. H. Gao, W. Z. Li, H. M. Li and X. Q. Qiu, *Ind Eng Chem Res*, 2020, **59**, 4367-4376.
10. G. Purohit, D. S. Rawat and O. Reiser, *Chemcatchem*, 2020, **12**, 569-575.
11. X. J. Cui, F. Shi and Y. Q. Deng, *Chemcatchem*, 2012, **4**, 333-336.
12. P. P. Zuo, J. Q. Duan, H. L. Fan, S. J. Qu and W. Z. Shen, *Appl Surf Sci*, 2018, **435**, 1020-1028.
13. S. Elangovan, C. Topf, S. Fischer, H. Jiao, A. Spannenberg, W. Baumann, R. Ludwig, K. Junge and M. Beller, *J Am Chem Soc*, 2016, **138**, 8809-8814.
14. R. Adam, C. B. Bheeter, J. R. Cabrero-Antonino, K. Junge, R. Jackstell and M. Beller, *ChemSuschem*, 2017, **10**, 842-846.
15. Z. Wei, J. Wang, S. Mao, D. Su, H. Jin, Y. Wang, F. Xu, H. Li and Y. Wang, *ACS Catalysis*, 2015, **5**, 4783-4789.
16. H. Alex, P. Loos, T. Baramov, J. Barry, T. Godiawala, J. Hassfeldt and N. Steinfeldt, *ChemCatChem*, 2017, **9**, 3210-

17. J. Liu, Y. Zhu, C. Wang, T. Singh, N. Wang, Q. Liu, Z. Cui and L. Ma, *Green Chemistry*, 2020, **22**, 7387-7397.
18. A. Jadhav, I. Ahmed, A. G. Baloch, H. Jadhav, S. Nizamuddin, M. T. H. Siddiqui, H. A. Baloch, S. S. Qureshi and N. M. Mubarak, *Biomass Conversion and Biorefinery*, DOI: 10.1007/s13399-019-00517-y.
19. K. Murugesan, T. Senthamarai, M. Sohail, A. S. Alshammari, M. M. Pohl, M. Beller and R. V. Jagadeesh, *Chemical Science*, 2018, **9**, 8553-8560.
20. A. Pei, L. N. Ruan, H. Fu, J. Liu, L. Zeng, H. Zhang, J. R. Hua, L. H. Zhu and B. H. Chen, *Crystengcomm*, 2020, **22**, 5382-5388.
21. X. Z. Zhuang, H. Zhan, Y. Q. Huang, Y. P. Song, X. L. Yin and C. Z. Wu, *Bioresource Technol*, 2018, **267**, 17-29.
22. X. Z. Zhuang, H. Zhan, Y. P. Song, C. He, Y. Q. Huang, X. L. Yin and C. Z. Wu, *Fuel*, 2019, **236**, 960-974.
23. X. Sun, A. I. Olivos-Suarez, L. Oar-Arteta, E. Rozhko, D. Osadchii, A. Bavykina, F. Kapteijn and J. Gascon, *ChemCatChem*, 2017, **9**, 1854-1862.
24. Z. L. Yuan, B. Liu, P. Zhou, Z. H. Zhang and Q. Chi, *Journal of Catalysis*, 2019, **370**, 347-356.
25. R. V. Jagadeesh, K. Murugesan, A. S. Alshammari, H. Neumann, M. M. Pohl, J. Radnik and M. Beller, *Science*, 2017, **358**, 326-+.
26. X. Y. Li, C. M. Zeng, J. Jiang and L. H. Ai, *J Mater Chem A*, 2016, **4**, 7476-7482.
27. W. J. Song, X. D. Yi, X. M. Jiang and W. K. Lai, *Ind Eng Chem Res*, 2020, **59**, 20298-20306.
28. S. B. Tian, M. Hu, Q. Xu, W. B. Gong, W. X. Chen, J. R. Yang, Y. Q. Zhu, C. Chen, J. He, Q. Liu, H. J. Zhao, D. S. Wang and Y. D. Li, *Science China-Materials*, 2021, **64**, 642-650.
29. Y. Y. Wang, Y. Liu, J. Y. Li, Y. Y. Liu, W. G. Zhang, M. M. Yang, Y. J. Jian, P. Zuo and Z. W. Gao, *Ind Eng Chem Res*, 2020, **59**, 11241-11249.
30. W. P. Han, S. M. Wang, X. K. Li, B. Ma, M. X. Du, L. G. Zhou, Y. Yang, Y. Zhang and H. Ge, *Rsc Adv*, 2020, **10**, 8055-8065.